




Pseudohypoxia in paraganglioma and pheochromocytoma is associated with an immunosuppressive phenotype

Lucía Celada^{1,2,3} , Tamara Cubiella^{1,2,3}, Jaime San-Juan-Guardado¹ , Gala Gutiérrez⁴, Brenda Beiguela⁴, Raúl Rodríguez⁵, María Poch⁵, Aurora Astudillo¹, Ana Grijalba⁶, Paula Sánchez-Sobrino⁷, María Tous⁸, Elena Navarro⁹, Teresa Serrano¹⁰, Miguel Paja¹¹, Nuria Valdés^{3,4*} and María-Dolores Chiara^{1,2,3*} 

¹ Institute of Sanitary Research of the Principado de Asturias, Oviedo, Spain

² CIBERONC (Network of Biomedical Research in Cancer), Madrid, Spain

³ Institute of Oncology of the Principado de Asturias, University of Oviedo, Oviedo, Spain

⁴ Department of Internal Medicine, Section of Endocrinology and Nutrition, Hospital Universitario de Cabueñes, Gijón, Spain

⁵ Department of Pathology, Hospital Universitario de Cabueñes, Gijón, Spain

⁶ Department of Clinical Analysis, Complejo Hospitalario de Navarra, Pamplona, Spain

⁷ Department of Endocrinology and Nutrition, Complejo Hospitalario de Pontevedra, Pontevedra, Spain

⁸ Department of Endocrinology and Nutrition, Hospital Universitario Virgen Macarena, Sevilla, Spain

⁹ Department of Endocrinology and Nutrition, Hospital Universitario Virgen del Rocío, Sevilla, Spain

¹⁰ Department of Pathology, Hospital de Bellvitge, Barcelona, Spain

¹¹ Department of Endocrinology and Nutrition, Hospital Universitario de Basurto, Bilbao, Spain

*Correspondence to: M-D Chiara, Institute of Sanitary Research of the Principado de Asturias, Av de Roma s/n, 33011-Oviedo, Spain. E-mail: mdchiara.uo@uniovi.es; N Valdés, Department of Internal Medicine, Section of Endocrinology and Nutrition, Hospital Universitario de Cabueñes, Los Prados, 395, 33394-Gijón, Spain. E-mail: nvaldes@hca.es

Abstract

Metastatic pheochromocytoma and paraganglioma (PPGL) have poor prognosis and limited therapeutic options. The recent advent of immunotherapies showing remarkable clinical efficacies against various cancer types offers the possibility of novel opportunities also for metastatic PPGL. Most PPGLs are pathogenically linked to inactivating mutations in genes encoding different succinate dehydrogenase (SDH) subunits. This causes activation of the hypoxia-inducible factor 2 (HIF2)-mediated transcriptional program in the absence of decreased intratumoral oxygen levels, a phenomenon known as pseudohypoxia. Genuine hypoxia in a tumor creates an immunosuppressive tumor microenvironment. However, the impact of pseudohypoxia in the immune landscape of tumors remains largely unexplored. In this study, tumoral expression of programmed death–ligand 1 (PD–L1) and HIF2 α and tumor infiltration of CD8 T lymphocytes (CTLs) were examined in PPGL specimens from 102 patients. We assessed associations between PD–L1, CTL infiltration, HIF2 α expression, and the mutational status of *SDH* genes. Our results show that high PD–L1 expression levels in tumor cells and CTL tumor infiltration were more frequent in metastatic than nonmetastatic PPGL. However, this phenotype was negatively associated with *SDH* mutations and high HIF2 α protein expression. These data were validated by analysis of mRNA levels of genes expressing PD–L1, CD8, and HIF2 α in PPGL included in The Cancer Genome Atlas database. Further, PD–L1 and CD8 expression was lower in norepinephrine than epinephrine-secreting PPGL. This *in silico* analysis also revealed the low PD–L1 or CD8 expression levels in tumors with inactivating mutations in *VHL* or activating mutations in the HIF2 α -coding gene, *EPAS1*, which, together with *SDH*-mutated tumors, comprise the pseudohypoxic molecular subtype of PPGL. These findings suggest that pseudohypoxic tumor cells induce extrinsic signaling toward the immune cells promoting the development of an immunosuppressive environment. It also provides compelling support to explore the differential response of metastatic PPGL to immune checkpoint inhibitors.

© 2022 The Authors. *The Journal of Pathology* published by John Wiley & Sons Ltd on behalf of The Pathological Society of Great Britain and Ireland.

Keywords: paraganglioma; pheochromocytoma; hypoxia; metastasis; programmed death–ligand 1; CD8-positive lymphocytes; succinate dehydrogenase; HIF2 α

Received 19 May 2022; Revised 10 October 2022; Accepted 27 October 2022

No conflicts of interest were declared.

Introduction

Hypoxia activates several adaptive responses, both in cancer and stromal cells, mainly mediated by the

hypoxia-inducible transcription factors HIF1 α and HIF2 α [1,2]. This results in cell cycle arrest, decrease of oxidative phosphorylation, increase of glycolysis, and angiogenesis. These reprogramming processes

contribute to tumor progression by supporting tumor cell survival and metastasis development [2].

The process wherein cells express oxygen-sensing genes in the absence of hypoxia is known as pseudohypoxia. Paraganglioma and pheochromocytoma (PPGL) are the prototype of tumors with a pseudohypoxic phenotype, especially the syndromic forms of disease mainly caused by inactivating mutations in *VHL*, encoding the von Hippel Lindau protein, or in genes encoding components of the succinate dehydrogenase (SDH) complex [3] such as *SDHB*, *SDHD*, *SDHC*, *SDHA*, or *SDHAF2*. Under normoxic conditions, HIF1 α /HIF2 α are hydroxylated in proline residues by the oxygen-dependent HIF prolyl-hydroxylase (PHD) enzymes. *VHL* protein binds selectively to hydroxylated HIF α subunits, targeting them for ubiquitination and proteasomal degradation. Under hypoxic conditions, PHD-activity is inhibited and non-hydroxylated HIF α subunits accumulate, dimerize with HIF1 β , and bind to hypoxia response elements in target genes to activate transcription [4]. Loss-of-function mutations of *VHL* prevent HIF α proteasomal degradation and thus promote the activity of HIF. Further, increased intracellular levels of the succinate oncometabolite, due to SDH loss of function, reduces PHD activity, induces the abnormal stabilization of HIF α in normoxia, and upregulates expression of HIF-target genes [5]. PPGL are also pathogenically associated with somatic gain-of-function mutations of *EPAS1*, the HIF2 α encoding gene [6]. In addition, HIF2 α , but not HIF1 α , is overexpressed in pseudohypoxic PPGL [7] and in *Sdhb* knockout-immortalized mouse chromaffin cells [8]. Thus, although the exact mechanism of PPGL tumor formation remains to be elucidated, proposed models include HIF2 α - rather than HIF1 α -dependent pseudohypoxic drive [9–12].

PPGL are generally slow-growing, indolent tumors, but approximately 20% of patients develop metastases, and once this occurs, the prognosis is poor and treatment options are rather limited [13]. The advent of immune checkpoint inhibitors (ICI) directed against programmed death protein 1 (PD-1) and its ligand (PD-L1) or cytotoxic T lymphocyte antigen 4 (CTLA-4) has revolutionized the treatment of many types of advanced cancers [14] and are being studied as therapeutic options for patients with metastatic PPGL [15]. Results from a first phase II clinical trial of pembrolizumab, an inhibitor of PD-1/PD-L1 interaction, was recently published showing a modest but variable antineoplastic activity with durable response in some patients [16]. This highlights the need to identify those patients with more chances of benefiting from these treatments and to be able to propose the most suitable combination therapies to boost the weak antitumor activities of ICI.

Overexpression of PD-L1 is a vital suppressor of antitumor immunity [17]. Most solid tumors with high expression of PD-L1 respond better to ICI targeting the PD-1/PD-L1 pathway [18]. Thus, the expression of PD-L1 remains one of the best biomarkers to predict response to ICI thus far. Another predictive marker of

response is related to the density and location of cytotoxic CD8 T lymphocytes (CTLs) within a tumor [19,20]. Tumors with high levels of CTL infiltration represent the best candidates for effective ICI-based monotherapy, whereas more approaches are needed in combination with ICI for tumors lacking intratumoral CTL. One of the most promising therapeutic approaches in those cases is a combination with agents intended to restore blood perfusion levels. This is because emerging evidence supports the idea that tumor hypoxia creates an immunosuppressive tumor microenvironment via activation of intrinsic mechanisms that allow tumor cells to escape innate and adaptive immune defenses, thereby opposing successful immunotherapy [21–23].

One of the driving forces behind immunosuppression in cancer is mediated by HIF1 α , which transcriptionally activates genes that block the infiltration and activity of CTL while stimulating the infiltration and activity of regulatory T cells, myeloid-derived suppressor cells, and tumor-associated macrophages [24,25]. Hypoxia also promotes the acidification of the microenvironment by secreted lactate and H⁺, which adversely affects the functionality of infiltrating T cells, resulting in tumor immune evasion [26–28]. Although the role of hypoxia and HIF1 α as a driving force of immunosuppressive tumor phenotypes is being resolved, it is unknown whether pseudohypoxic tumor cells also suppress tumor immunity. This is especially intriguing in PPGL where, as indicated earlier, activation of pseudohypoxia is mediated by HIF2 α , rather than HIF1 α [7,11]. Moreover, in contrast to truly hypoxic tumors, the HIF-activated transcriptional program in PPGL occurs in tumor cells harboring genetic inactivation of *VHL* or *SDH* genes but not in the infiltrated immune cells.

Only two previous studies explored the expression of PD-L1 protein in PPGL [29,30]. They showed that PD-L1 correlated with the Ki-67 proliferation biomarker but not with metastatic disease. However, the relationship between PD-L1 and the genetic base of the disease remains to be fully documented. Nor is it known whether CTLs infiltrate PPGL. In this report, we aimed to define and compare the immune landscape of PPGL with their pseudohypoxic profile, genotypic origin, and metastatic behavior to provide helpful information for their targeted treatment.

Materials and methods

Tumor samples

Tumor specimens of formalin-fixed and paraffin-embedded (FFPE) ($n = 111$) tissues were obtained from 102 patients with PPGL, diagnosed and treated between 1986 and 2016 at the following hospitals: Central de Asturias, Cabueñes, Virgen del Rocío, Virgen Macarena, Bellvitge, Basurto, Navarra, and Pontevedra (Spain). Tumor samples included 103 primary tumors and eight metastases. Informed consent was obtained from each patient. Thirty patients were diagnosed with

metastatic disease developed at sites where chromaffin cells were physiologically absent [31]. The study was approved by the ethical committee of each hospital. The methods were carried out in accordance with the approved guidelines and the principles expressed in the Declaration of Helsinki. Clinical data were collected from patients' medical reports. The gene mutation data were retrieved from our previous studies [32–34].

Immunohistochemistry

FFPE human tumor tissue blocks were cut into 4- μ m sections and mounted on poly-L-lysine-coated slides. Antigen retrieval was performed using a high pH EnVision™ FLEX target retrieval solution for 20 min in a Dako PT link platform (Dako Denmark A/S, Glostrup, Denmark), followed by staining with a Dako EnVision™ Flex detection system. Tissue sections were incubated with primary antibodies against PD-L1 (rabbit IgG anti-PD-L1 clone E1L3N, dilution 1:200, Cell Signaling Technology, Danvers, MA, USA), CD8 (mouse anti-human CD8 clone C8/144B, prediluted, Dako), SDHB (rabbit anti-SDHB polyclonal, dilution 1:800, Sigma-Aldrich, St. Louis, MO, USA), and HIF2 α (rabbit IgG anti-HIF2 α polyclonal ab199 lot number: GR3374543-1, dilution 1:50, Abcam, Cambridge, UK). Positive and negative controls were also included. Results were evaluated randomly by AA, LC, RR, MP, and MDC without knowledge of clinical information. HIF2 α immunostaining (either nuclear or cytoplasmic), performed in 16 samples, were defined as positive (strong or weak immunostaining) or negative (absence of any immunostaining). PD-L1 immunostaining was evaluated as positive when all tumor cells or any percentage of them showed membrane immunostaining. Regarding CD8, following established immunoscores [35], we classified tumors as CD8 positives when immunostaining of immune cells was found in >20% of the tumor tissue. Tumors lacking CTLs were considered to have an immune-negative phenotype. Immune-negative tumors were also considered to be those with immunosuppressive phenotype, defined by poor (<20% infiltrative CTL), not absent, CTL infiltration ('altered-immunosuppressive') or by the presence of CTL at the borders of the tumor or the stroma surrounding the tumor nests, but that were not infiltrating the tumor ('altered-excluded'). The altered phenotypes reflect the ability of the tumor to escape T cell-mediated immune response by creating an ecosystem that hinders their infiltration. PD-L1 and CD8 immunohistochemistry was performed in 102 and 81 tumor samples, respectively, with an overlap of 72 samples that could be analyzed with both antibodies (66 primary tumors and six metastasis). Data from SDHB immunohistochemistry ($n = 21$) were obtained from our previous reports [32–34]. The number of samples analyzed with each antibody is shown in the supplementary material (Figure S1).

The Cancer Genome Atlas data analysis

RNAseq data from PPGL were retrieved from The Cancer Genome Atlas (TCGA) data portal (<https://tcga-data.nci.nih.gov/tcga/>). This included gene expression profiles of 184 primary tumors of which 33 had a pseudohypoxic molecular profile, defined here as those carrying mutations in *VHL* (seven with germline mutations and three with somatic mutations), *SDH* (12 with germline *SDHB* mutations and three with *SDHD* mutations), or *EPAS1* (eight with somatic mutations) genes. This dataset shows gene-level transcript estimates, as in $\log_2(x + 1)$ transformed RSEM normalized counts. mRNA levels of *CD274*, *CD8A*, *TCF7*, *CD56*, *EPAS1*, *LDHA*, and *PNMT* were dichotomized as high or low according to their expression levels being above or below the median value.

Statistical analyses

All statistical data were produced using SPSS 20.0 (IBM, Armonk, NY, USA) and GraphPad Prism 6.0 (GraphPad Software Inc., San Diego, CA, USA). The association between PD-L1 and CD8 and clinicopathological characteristics was analyzed with a χ^2 test or Mann–Whitney *U*-test. All statistical results with a *P* value < 0.05 were considered to be significant.

Results

Higher prevalence of PD-L1 expression and CTL tumor infiltration in metastases and in metastatic versus nonmetastatic primary PPGL

The expression of PD-L1 and CD8 was analyzed by immunohistochemistry in a cohort of 102 patients with PPGL (111 tumor samples: 103 primary tumors and eight metastases). The clinical characteristics of the patients are shown in Table 1. About 50% of primary tumors derived from parasympathetic head and neck paraganglia and the rest arose at sympathetic paraganglia, i.e. the adrenal medulla or abdominal paraganglia. Patients were followed up over a median period of 8 years (range 1–35 years). Thirty patients were diagnosed with metastatic disease. Forty-two patients had mutations in any of the genes encoding *SDH* protein subunits, four patients had mutation in *VHL*, two in *NFI*, and one in *HRAS*.

PD-L1 positive immunostaining was exclusively localized in tumor cells, not stromal cells, with cytoplasmic and plasma membrane staining (Figure 1). It was detected in 16.7% of samples: 12.7% (12/94) of primary PPGL (primPPGL) and 62.5% and (5/8) of metastatic tissues (Figure 2).

CTL densely infiltrating the tumor tissue was detected in 19.7% of tumor samples [16% (12/75) of primPPGL and 66.6% (4/6) of metastatic tissues], whereas the remaining tumors (~80%) had an immunosuppressive phenotype (Figure 2). Following published recommendations [35], and as indicated in the "Materials and methods" section, tumors with immunosuppressive

Table 1. Clinical data of patients in association with PD-L1 and CD8 immunostaining.

| | PD-L1 | | CD8 | | |
|----------------|----------|----------|-----------------|--------------------------|----|
| | Positive | Negative | Positive (high) | Negative (cold/excluded) | |
| Tumor location | | | | | |
| HNPGL | 55 | 4 | 44 | 5 | 29 |
| PCC/PGL | 48 | 8 | 38 | 7 | 34 |
| Metastasis | 8 | 5 | 3 | 4 | 2 |
| Gender | | | | | |
| Female | 55 | 6 | 45 | 6 | 35 |
| Male | 50 | 11 | 35 | 9 | 28 |
| Unknown | 6 | | | | |
| Age | | | | | |
| <45 years | 37 | 3 | 30 | 4 | 24 |
| >45 years | 55 | 8 | 42 | 4 | 33 |
| Unknown | 19 | | | | |
| Genotype | | | | | |
| <i>SDHB</i> | 26 | 4 | 19 | 1 | 19 |
| <i>SDHD</i> | 15 | 1 | 12 | 1 | 7 |
| <i>SDHA</i> | 1 | 0 | 1 | 0 | 1 |
| <i>VHL</i> | 4 | 1 | 3 | 2 | 1 |
| <i>NF1</i> | 2 | 0 | 2 | 1 | 1 |
| <i>HRAS</i> | 1 | 0 | 1 | 0 | 1 |
| None | 50 | 10 | 36 | 9 | 29 |
| Unknown | 12 | | | | |
| MPPGL | | | | | |
| No | 73 | 4 | 62 | 5 | 44 |
| Yes | 38 | 13 | 23 | 11 | 21 |

Notes: HNPGL, head and neck paraganglioma; PCC/PGL, pheochromocytoma/paraganglioma; MPPGL, primary tumors that developed metastasis ($n = 30$) + metastatic tissues ($n = 8$).

phenotype included those having an altered-excluded phenotype (9% of cases) or a cold phenotype (71% of cases). Representative immunohistochemical images are shown in Figure 1. Significantly, 60% of tumors with high levels of infiltrating CTL also displayed high levels of tumor cells with PD-L1 positive immunostaining ($P < 0.0001$, Figure 2).

Our sample collection included 30 primPPGL that had been diagnosed with either synchronous (28 cases) or metachronous (two cases) metastasis, which allowed us to compare the levels of PD-L1 expression and CTL infiltration in metastatic primPPGL and PPGL that had not developed metastasis up to the last date of follow-up. This analysis revealed that the prevalence of PD-L1 expression or high CTL infiltration was higher in metastatic than nonmetastatic primPPGL: 8/28 (28.6%) versus 4/66 (6%), $P = 0.005$ for PD-L1, and 7/26 (27%) versus 5/49 (10.2%), $P = 0.063$ for CTL infiltration (Figure 2). The heightened PD-L1 expression and CTL infiltration in metastatic primPPGL could be explained by a higher number of neoantigens associated with increased tumor mutational burden (TMB) in these tumors. Although moderated, analysis of the PPGL included in the TCGA database confirmed that metastatic PPGL have increased TMB in comparison with nonmetastatic PPGL (Figure 2, $P < 0.0001$).

Collectively, these data revealed a higher prevalence of PD-L1 expression and CTL infiltration in both, metastases, and primPPGL diagnosed with synchronous or metachronous metastasis than in nonmetastatic

primPPGL (36% versus 6%, $P < 0.0001$ for PD-L1 and 34.4% versus 10.2%, $P = 0.009$ for CTL infiltration).

PD-L1 expression and CTL tumor infiltration in relationship with sympathetic and parasympathetic origin of PPGL

Our cohort included paraganglioma of parasympathetic origin (head and neck paraganglioma, hereafter pPPGL) and sympathetic origin (pheochromocytoma and abdominal paraganglioma, hereafter sPPGL). All metastatic tissues were of sympathetic origin, and only 3/30 metastatic primPPGL were of parasympathetic origin. We determined whether there was any association between the immune phenotypes and the organ of origin of primPPGL. PD-L1 overexpression was found more frequently in sPPGL (8/46; 17.4%) than in pPPGL (4/48; 8%). CTL infiltration was found in 7/41 (17%) sPPGL and 5/34 (14%) pPPGL (Figure 3). We confirmed that PD-L1 expression and CTL infiltration was more frequent in metastatic than nonmetastatic primPPGL when the analysis was restricted to sPPGL, excluding pPPGL (Figure 3): 7/25 (28%) metastatic primPPGL had increased PD-L1 expression versus 1/21 (4.7%) nonmetastatic primPPGL ($P = 0.043$). In addition, 6/23 (26%) metastatic primPPGL had increased CTL infiltration versus 1/18 (5%) nonmetastatic primPPGL ($P = 0.092$).

Although the number of metastatic pPPGL was very small in terms of delivering any statistically significant results, we also observed that PD-L1 expression and CTL infiltration were more frequent among metastatic than nonmetastatic primPPGL (Figure 3): PD-L1 was expressed in 1/3 (33%) metastatic versus 3/45 (6%) nonmetastatic primPPGL ($P = 0.234$) and CTL infiltration was found in 1/3 (33%) metastatic versus 4/31 (12.9%) nonmetastatic primPPGL ($P = 0.389$).

Given that metastases and metastatic primPPGL are the potential targets of therapies with ICI, we next focused our analysis on these tumors (hereafter abbreviated as MPPGL).

Low prevalence of PD-L1 expression and CTL tumor infiltration in MPPGL with *SDH* mutations

SDH-mutated PPGL are known to have a pseudohypoxic phenotype. To test whether pseudohypoxia has an impact on the immune landscape of tumors, we analyzed the association between the immune phenotypes of tumors and their genetic background. We found that 10/17 (59%) *SDH*-wild type MPPGL had increased PD-L1 expression versus 3/14 (21.4%) of *SDH*-mutated tumors ($P = 0.040$) (Figure 4). In addition, CTL infiltration was significantly more frequent in tumors lacking *SDH* mutations than in *SDH*-mutated MPPGL [9/16 (56.2%) versus 1/13 (7.7%); $P = 0.008$] (Figure 4).

Genetic inactivation of *SDH* genes can be detected by the loss of *SDHB* protein immunostaining [36]. Because *SDH* mutations can also arise at somatic, not germline, levels, we retrieved *SDHB* immunohistochemical data from our previous reports [32–34] in 21 MPPGL samples

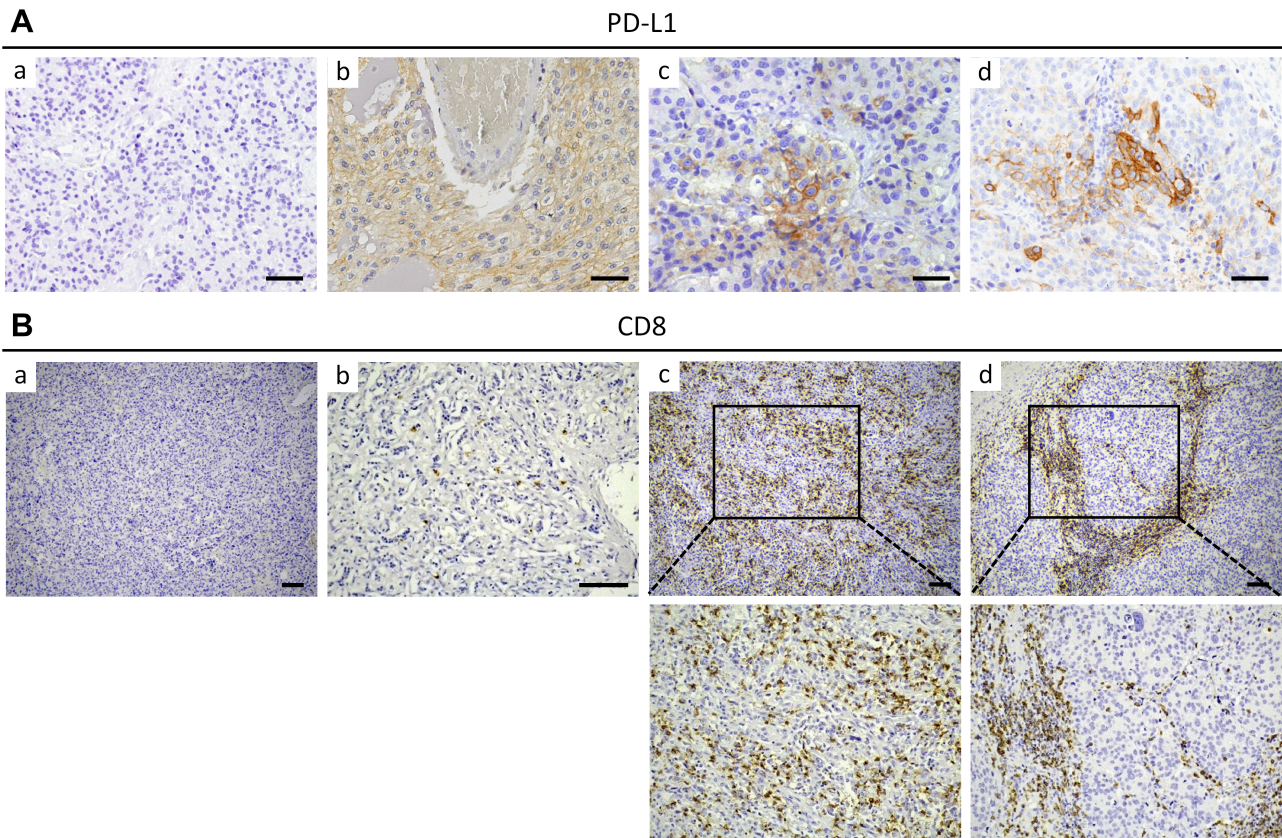


Figure 1. PD-L1 and CTL expression in PPGL. (A) Representative images of PD-L1 immunohistochemistry performed in PPGL showing absence (a) or presence of homogenously (b) or focally (c and d) distributed staining of PD-L1. Positive immunostaining is localized at plasma membrane and cytoplasm of tumor cells. Scale bars, 50 μ m. (B) Representative images of CD8 immunohistochemistry performed in PPGL showing tumors with cold (a and b), hot (c), or immune-excluded (d) phenotypes. Images below (c) and (d) are magnified pictures of the areas outlined in (c) and (d), respectively. Scale bars, 100 μ m.

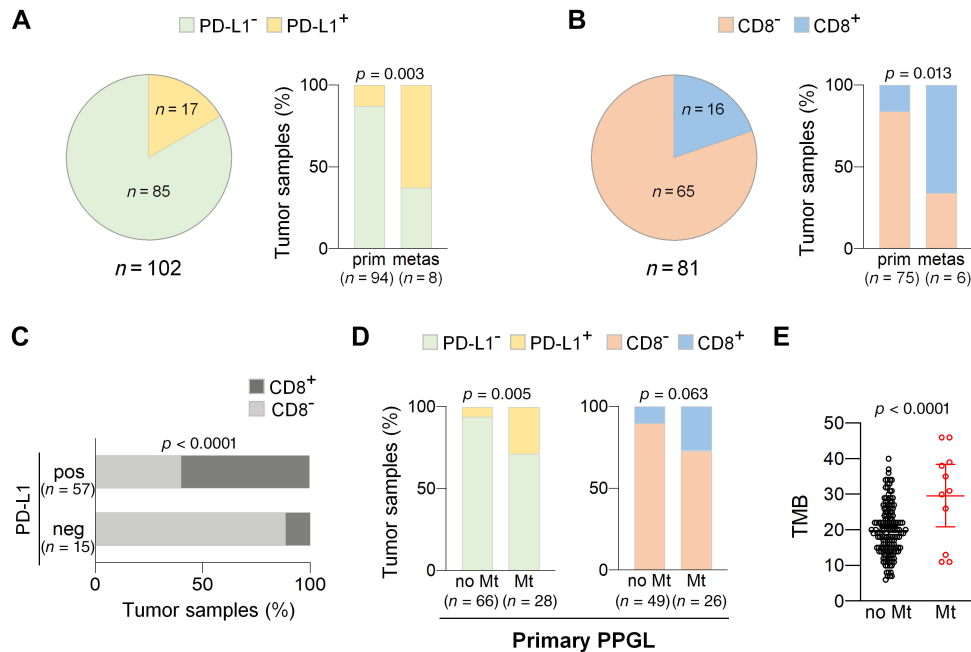


Figure 2. High PD-L1 expression and CTL tumor infiltration in metastases and metastatic primPPGL. (A and B) Charts showing percentage of tumor samples with (A) negative or positive PD-L1 or (B) CD8 immunostaining. Pie charts include analysis of primPPGL and metastases. Bar charts include analysis of samples categorized as primPPGL (prim) or metastases (metas). (C) Bar charts showing percentage of samples with negative (neg) or positive (pos) PD-L1 expression that have high or low CTL tumor infiltration. (D) Bar charts showing percentage of tumor samples with (PD-L1⁺, CD8⁺) or without (PD-L1⁻, CD8⁻) PD-L1 expression or CTL infiltration in metastatic (Mt) and nonmetastatic (no Mt) primPPGL. Total number of tumors in each group is indicated in parentheses in A–D. (E) Tumor mutation burden (TMB) in metastatic (Mt) and nonmetastatic (no Mt) PPGL included in TCGA dataset.

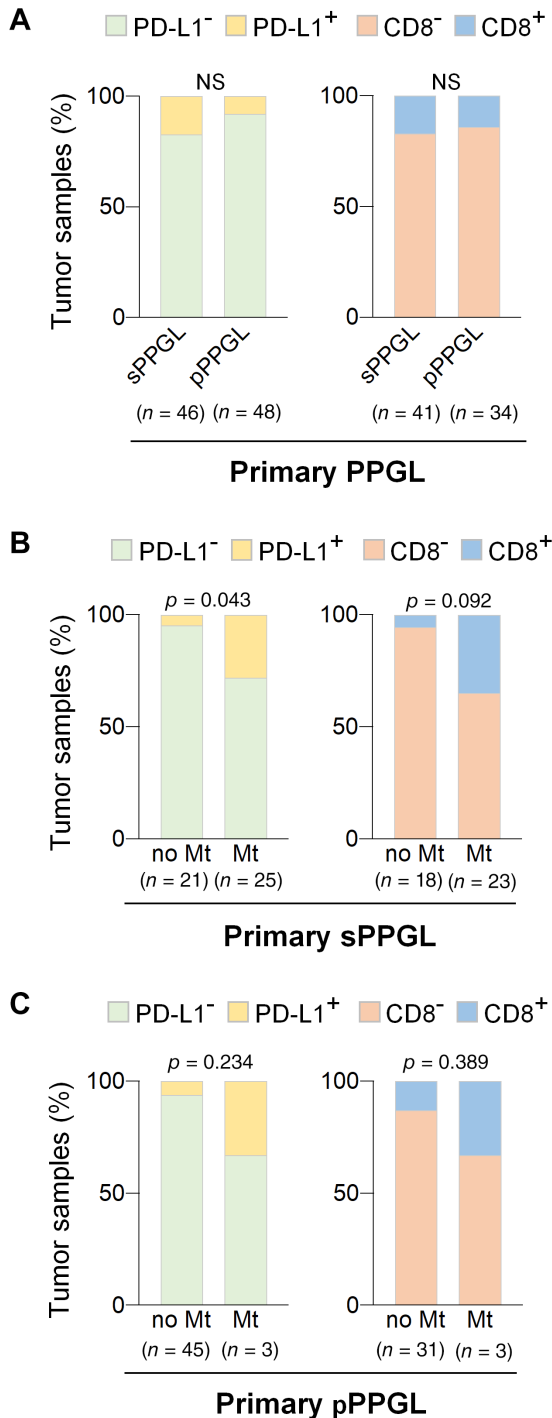


Figure 3. PD-L1 and CTL expression in sympathetic and parasympathetic PPGL. (A) Bar charts showing percentage of tumor samples with (PD-L1⁺, CD8⁺) or without (PD-L1⁻, CD8⁻) PD-L1 expression or CTL infiltration in sympathetic primPPGL (sPPGL) and parasympathetic (pPPGL) primPPGL. (B and C) Bar charts showing percentage of tumor samples with (PD-L1⁺, CD8⁺) or without (PD-L1⁻, CD8⁻) PD-L1 expression or CTL infiltration in metastatic (Mt) and nonmetastatic (no Mt) tumors: (B) sPPGL and (C) pPPGL. Total number of tumors in each group is indicated in parentheses.

to compare SDHB protein expression, PD-L1, and CTL. As shown in Figure 4, PD-L1 expression was more frequent in SDHB-positive than negative tumors [8/12 (66.6%) versus 1/9 (11%); $P = 0.016$]. In addition, high levels of CTL infiltration were found in 9/12 (75%)

SDHB-positive tumors but not in any of the tumors with negative SDHB immunostaining ($P = 0.001$) (Figure 4).

Low prevalence of PD-L1 expression and CTL tumor infiltration in MPPGL overexpressing HIF2 α

PPGL with inherited mutations in *SDH* genes have a genetically determined pseudohypoxic phenotype. Therefore, we examined the association of the immune phenotype of PPGL and expression of HIF2 α , the master regulator of hypoxia signaling in PPGL.

Analysis of HIF2 α protein expression in 15 MPPGL tumor samples allowed us to confirm our previously reported data [7] showing that HIF2 α protein expression was positively associated with *SDH* mutations ($P = 0.006$) (Figure 5). We also found that the prevalence of tumors expressing PD-L1 or with CTL infiltration was higher among tumors with negative than positive HIF2 α immunostaining (Figure 5): 6/7 (85.7%) versus 1/9 (11%) expressed PD-L1 ($P = 0.006$) and 5/7 (71.4%) versus 1/7 (14.3%) had immunosuppressive phenotype ($P = 0.051$) (Figure 5).

Analysis of immune phenotype of MPPGL and clinical variables

We found no significant association between PD-L1 expression and sex (3/13 females and 10/19 males had PD-L1 expression; $P = 0.095$) or age of patients (3/8 patients <45 years and 5/17 patients >45 years had PD-L1 expression, $P = 0.513$). Regarding CTL infiltration levels, we found a statistically significant association with sex (1/13 females and 9/17 males had increased CTL infiltration, $P = 0.011$) but not age (2/9 patients <45 years and 2/14 patients >45 years had increased CTL infiltration, $P = 0.517$). Nevertheless, it should be noted that 8/9 (89%) males and 1/1 (100%) of females with CTL infiltration lacked *SDH* mutations.

High CTL infiltration levels were associated with shorter time to disease progression ($P = 0.030$) but not with disease survival ($P = 0.130$). However, multivariate Cox analysis of CTL and *SDH* mutations indicated that CTL infiltration levels were not a prognostic factor for PPGL ($P = 0.084$). No associations were found between CTL and overall survival ($P = 0.296$) or between PD-L1 expression and disease survival ($P = 0.636$) or time to progression ($P = 0.407$).

Validation and extended data supporting the association of an immunosuppressive phenotype with pseudohypoxia

The immunohistochemistry analysis provided data restricted to a single section of the tumors and did not inform on the immune profile of the bulk of the tumor mass. In addition, we were unable to detect PD-L1 or CD8 by immunostaining in most nonmetastatic samples, suggesting that these proteins were not expressed in those samples or that their levels were not high enough to be detected by immunohistochemistry. These facts

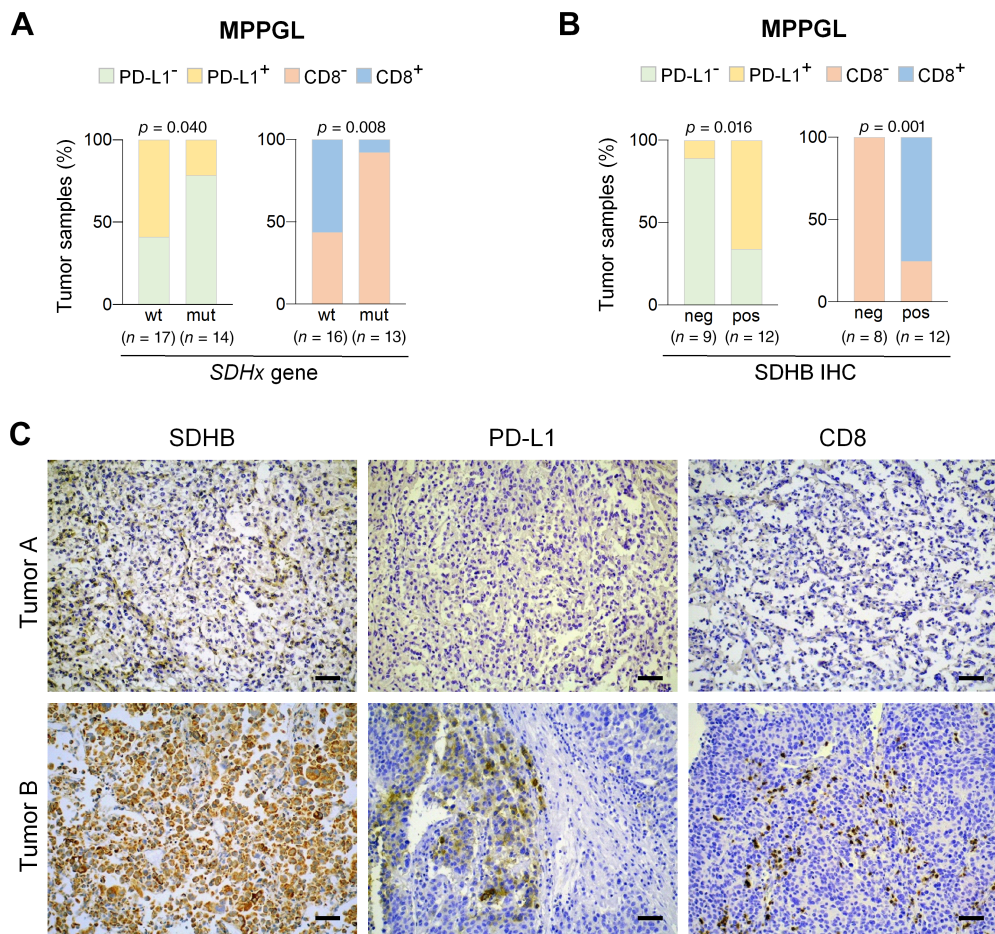


Figure 4. Immunosuppressive phenotype of MPPGL carrying *SDH* mutations. (A and B) Bar charts showing (A) percentage of tumor samples with (PD-L1⁺, CD8⁺) or without (PD-L1⁻, CD8⁻) PD-L1 expression or CTL infiltration in MPPGL that carried (mut) or not (wt) *SDH* mutations or (B) displayed negative (neg) or positive (pos) SDHB immunostaining. Total number of tumors in each group is indicated in parentheses. (C) Representative immunohistochemical images of two MPPGL samples showing that loss of SDHB protein expression is associated with low CD8 and PD-L1 immunostainings. Scale bars, 50 μ m.

prevented us from testing the hypothesis of whether there was an association between the immune phenotype and pseudohypoxia beyond the aggressiveness of the tumors. Thus, we resorted to the RNAseq data of the PPGL included in the TCGA database to analyze PD-L1, CD8, and HIF2 α expression at the mRNA level.

Increased *EPAS1* mRNA levels are a feature of pseudohypoxic PPGL [7]. We found that high levels of expression of *CD274* or *CD8A* genes, encoding PD-L1 and CD8, respectively, were associated with low *EPAS1* (encoding HIF2 α) mRNA levels ($P < 0.0001$ and $P = 0.009$, respectively) (Figure 6). A similar association was found between *EPAS1* and other lymphocyte markers such as *TCF7* or *CD56* (Figure 6).

To determine whether tumors with low expression levels of *CD274* or *CD8A* had higher HIF2 α activity, we queried known metrics of HIF2 α activity. HIF2 α activity is associated with increased *LDHA* gene expression and decreased expression of phenylethanolamine *N*-methyltransferase (*PNMT*), which catalyzes methylation of norepinephrine to form epinephrine. Consequently, reduced epinephrine synthesis is a hallmark of SDH-deficient tumors, as shown in Figure 6. We found that *CD274*, *CD8A*, *TCF7*, and

CD56 overexpressions were associated with increased levels of *PNMT* but decreased levels of *LDHA*. Further, epinephrine-secreting PPGL expressed higher levels of *CD274*, *CD8A*, *TCF7*, and *CD56* than tumors secreting norepinephrine (Figure 6).

We confirmed that *SDH*-mutated PPGL had lower expression levels of *CD274* and *CD8A* than tumors lacking *SDH* mutations or harboring mutations in other PPGL-related genes (Figure 6). The TCGA cohort includes tumors with genetic alterations affecting other genes involved in oxygen sensing, such as inactivating mutations of *VHL* or activating mutations of *EPAS1*. Interestingly, these pseudohypoxic tumors also expressed lower levels of *CD274* and *CD8A* than tumors harboring mutations in other genes (Figure 6).

The TCGA database includes PPGL that activate the pseudohypoxic transcriptome in the absence of mutations in the oxygen-sensing genetic machinery via, apparently, nongenetic mechanisms. These represent 39% of all pseudohypoxic PPGL. In addition, the TCGA database contained three other molecular subtypes of PPGL: Wnt-altered (associated with genetic alterations in *CSDE1* or *MAML3*), kinase-signaling (due to mutations in *RET*, *NF1*, *TMEM127*, *MAX*, *HRAS*, *FGFR1*, *MET*), or cortical

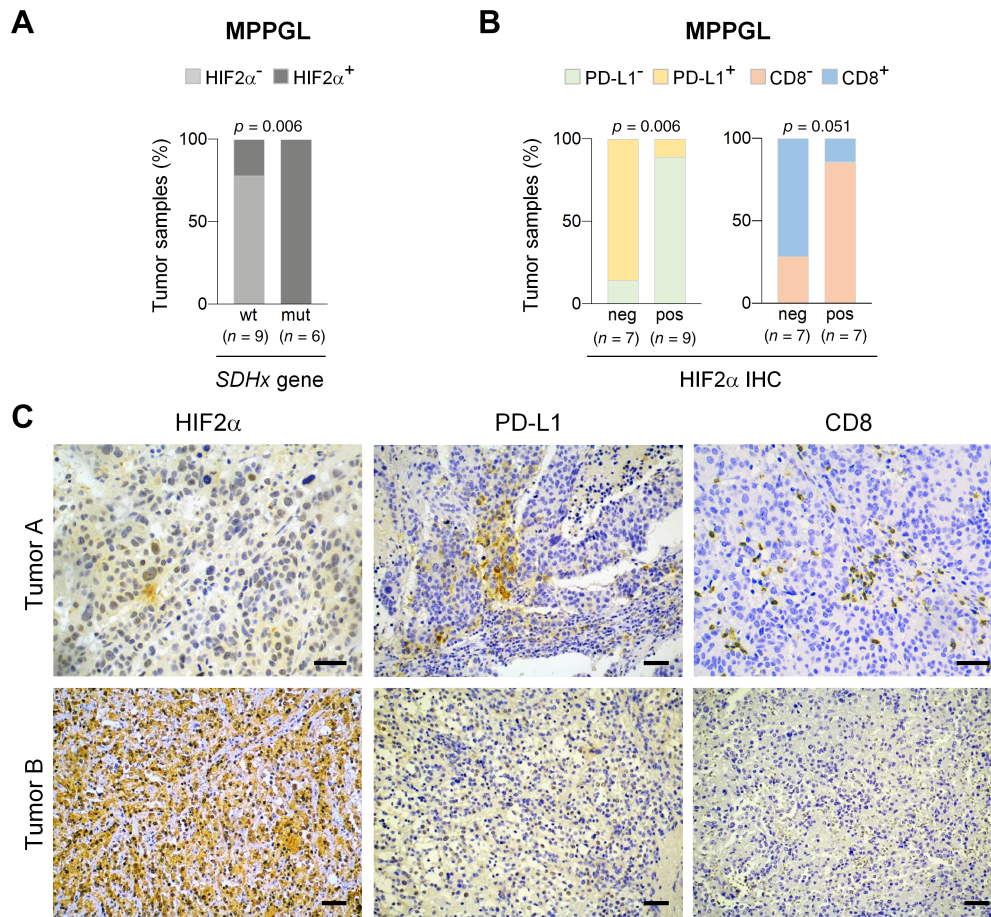


Figure 5. Immunosuppressive phenotype of MPPGL overexpressing HIF2α. (A) Bar charts showing percentage of tumors with wild-type (wt) or mutant (mut) *SDH* that have positive (HIF2α⁺) or negative (HIF2α⁻) HIF2α protein expression. (B) Bar charts showing relationship between negative (neg) or positive (pos) HIF2α immunostaining and expression of PDL-L1 or CD8 in MPPGL. Total number of tumors in each group is indicated in parentheses in (A) and (B). (C) Representative immunohistochemical images of two MPPGL samples showing that positive HIF2α protein expression is associated with low CD8 and PD-L1 immunostainings. Scale bars, 50 μm.

admixture. Comparison of *CD274* expression in all pseudohypoxic PPGL (genetically and nongenetically determined) and the other subtypes of PPGL confirmed that pseudohypoxic PPGL had the lowest levels of expression ($P < 0.0001$) (Figure 6). *CD8A* mRNA levels were lower in pseudohypoxic-PPGL than kinase- or cortical admixture-PPGL but similar to those of PPGL with Wnt-altered molecular signature.

Discussion

Here, we analyzed the immune landscape of PPGL in relation to their molecular phenotype, genotype, and metastatic behavior. The immunological phenotype in PPGL has been largely unexplored, likely because of the frequent benign behavior of these tumors and low TMB, suggesting that they do not accumulate neoantigens. However, approximately 10–20% of PPGL can develop into metastatic cancer, for which there are extremely limited therapeutic options. Recently developed ICI may offer new therapeutic opportunities for this disease. In fact, a first clinical trial revealed that some patients with metastatic PPGL

gained a moderated but, in some cases, durable clinical benefit when treated with pembrolizumab [16,37]. Knowledge of CTL tumor infiltration and PD-L1 expression levels in PPGL are the basis for ICI-based therapies. However, to date, the level of infiltration of CTL in PPGL has not been reported, and only two previous reports explored PD-L1 expression in these tumors [29,30]. Here, we report for the first time that about 35% of MPPGL had high PD-L1 levels and CTL infiltration. In contrast, CTL infiltration and PD-L1 expression are quite infrequent in nonmetastatic forms of PPGL in which infiltrating CTLs were found in only 10% of tumors. Importantly, we also show for the first time that 64% of metastatic tissues have high CTL infiltration. Taken together, the data support the notion that MPPGL could be a potential target for ICI-based therapies. However, we found that 70% of MPPGL had a cold immune phenotype and low or no PD-L1 expression, and 35% of metastasis did not accumulate CTL or not expressed PD-L1. Our analysis of phenotype–genotype correlations revealed that the cold-immune phenotype in those MPPGL was in fact associated with the presence of *SDH* mutations, suggesting that *SDH* deficiency–driven pseudohypoxia

may create an immunosuppressive tumor ecosystem in MPPGL.

Tumor hypoxia is known to impair the efficacy of PD-1/PD-L1 blockade by reducing CTL infiltration, among other reasons [22,38,39]. However, how pseudohypoxia impacts the immune landscape of tumors was not previously known. It should not be assumed that there is a parallelism between hypoxia and pseudohypoxia. Tumor cell-intrinsic loss of function of the *SDH* or *VHL* activity triggers a pseudohypoxic molecular response that, in contrast to hypoxic solid tumors, specifically occurs in genetically modified tumor cells but not in the surrounding tumor immune microenvironment. In addition, PPGL are, generally, highly vascularized and, consequently, not hypoxic tumors. Thus, the PPGL provides the opportunity to determine whether it is the sensing of decreased oxygen levels in the whole tumor microenvironment or the pseudohypoxia that creates an immunosuppressive ecosystem. Our findings suggest that tumor cell-intrinsic pseudohypoxia may drive an immunosuppressive phenotype in pseudohypoxic PPGL given that a cold or altered-excluded phenotype was more frequently found in tumors with *SDH* mutations, high levels of HIF2 α , and an absence of SDHB compared with tumors that lack *SDH* mutations, do not accumulate HIF2 α , and express physiological levels of SDHB protein. A previous report claimed no association of PD-L1 expression and HIF in PPGL [30]. However, that study analyzed HIF1 α as a pseudohypoxia biomarker that, in contrast to HIF2 α , does not distinguish between *SDH*-mutated and *SDH*-wild-type tumors [32,40].

We further show that the immunosuppressive phenotype is associated with HIF2 α activity as shown by the negative and positive association of *CD8A* (or *CD274*) with *PNMT* and *LDHA* mRNA levels, respectively. The *LDHA* gene is a direct target of HIF2 α and an important mediator of immunosuppression, as demonstrated in recent reports. Kumagai *et al.* revealed lactic acid as a mediator of checkpoint blockade resistance [41]. It promotes T regulatory cell immunosuppressive activity and impairs CTL function [26,27]. This observation provides a plausible explanation for the immunosuppressive environment of pseudohypoxic PPGL. Nevertheless, the scenario may be more complex since, although T cells are the primary effectors of the antitumor response, mounting evidence demonstrates that innate immune cells are critical to successful tumor clearance [42]. Hypoxia induces changes in the metabolic pathways that drive innate immune cells toward immune activation or suppression [43]. Thus, it will also be key to define the role of the innate immune system in pseudohypoxic MPPGL.

Collectively, our data suggest that pseudohypoxic tumor cells induce extrinsic signaling toward the immune system, inducing the development of an immunosuppressive environment. This suggests that a combination with therapeutic strategies targeting the HIF2 α activity would enhance antitumor immunity and maximize the clinical benefit of immunotherapy in these tumors [44,45]. Intriguingly, loss of HIF-2 α has been shown to render immune suppressor Treg cells

functionally defective, suggesting that HIF2 α inhibition could enhance T cell-mediated antitumor cytotoxicity [46]. Belzutifan, a potent and selective small-molecule inhibitor of HIF2 α , has demonstrated a remarkable therapeutic benefit for patients with clear cell renal cell carcinoma and the Pacak–Zhuang syndrome caused, respectively, by loss-of-function mutations in *VHL* or gain-of-function mutations in *EPAS1* [47,48]. A phase II clinical trial is under way for the treatment of advanced PPGL with belzutifan (NCT04924075), and other clinical trials are investigating the efficacy of combinatorial treatment methods, including belzutifan with ICI in advanced renal carcinoma, which is another type of pseudohypoxic tumor linked to *VHL* mutations and HIF2 α activation [49]. Our study provides a rationale for the development of similar therapeutic approaches for MPPGL, particularly for pseudohypoxic tumors.

Taken together, we report here for the first time that pseudohypoxic MPPGL has an immunosuppressive phenotype. These data could help in the design of combined immunotherapeutic approaches in pseudohypoxic MPPGL.

Acknowledgements

This research was funded by Instituto de Salud Carlos III through Project PI20/01754 (cofunded by European Regional Development Fund/European Social Fund ‘A way to make Europe’/‘Investing in your future’), the Centro de Investigación Biomedica en Red-Cancer, CIBERONC, the Grupo Español de Tumores Huérfanos e Infrecuentes (GETHI), the PHEiPAS Association, and the Principado de Asturias and European Regional Development Fund through Project IDI/2021/00079. LC thanks the Spanish Ministerio de Ciencia, Innovación y Universidades for a FPU predoctoral contract. TC thanks Consejería de Ciencia, Innovación y Universidad (Principado de Asturias) for a Severo-Ochoa predoctoral contract.

Author contributions statement

MDC conceptualized the study. LC, TC, AA, RR, MP and JS-J-G contributed to the methodology. MDC, NV and LC performed formal analysis. MDC, NV, LC, GG, BB, AG, PS-S, MT, EN, TS and MP performed data curation. MDC contributed to writing and MDC, NV, LC and TC to writing, review, and editing. MDC and LC contributed to visualization. MDC and NV obtained funding. All authors have read and agreed to the published version of the manuscript.

Data availability statement

The raw TCGA data are available for download from TCGA data portal (<https://tcga-data.nci.nih.gov/tcga/>).

References

- Kim LC, Simon MC. Hypoxia-inducible factors in cancer. *Cancer Res* 2022; **82**: 195–196.
- Schito L, Semenza GL. Hypoxia-inducible factors: master regulators of cancer progression. *Trends Cancer* 2016; **2**: 758–770.
- Crona J, Lamarca A, Ghosal S, et al. Genotype-phenotype correlations in pheochromocytoma and paraganglioma: a systematic review and individual patient meta-analysis. *Endocr Relat Cancer* 2019; **26**: 539–550.
- Kaelin WG, Ratcliffe PJ. Oxygen sensing by metazoans: the central role of the HIF hydroxylase pathway. *Mol Cell* 2008; **30**: 393–402.
- Selak MA, Armour SM, MacKenzie ED, et al. Succinate links TCA cycle dysfunction to oncogenesis by inhibiting HIF- α prolyl hydroxylase. *Cancer Cell* 2005; **7**: 77–85.
- Zhuang Z, Yang C, Lorenzo F, et al. Somatic HIF2A gain-of-function mutations in Paraganglioma with polycythemia. *N Engl J Med* 2012; **367**: 922–930.
- Celada L, Cubiella T, San-Juan-Guardado J, et al. Differential HIF2 α protein expression in human carotid body and adrenal medulla under physiologic and tumorigenic conditions. *Cancers* 2022; **14**: 2986.
- Morin A, Goncalves J, Moog S, et al. TET-mediated Hypermethylation primes SDH-deficient cells for HIF2 α -driven mesenchymal transition. *Cell Rep* 2020; **30**: 4551–4566.e7.
- Vaidya A, Flores SK, Cheng Z-M, et al. EPAS1 mutations and Paragangliomas in cyanotic congenital heart disease. *N Engl J Med* 2018; **378**: 1259–1261.
- Toledo RA, Qin Y, Srikantan S, et al. In vivo and in vitro oncogenic effects of HIF2A mutations in pheochromocytomas and paragangliomas. *Endocr Relat Cancer* 2013; **20**: 349–359.
- Eisenhofer G, Huynh TT, Pacak K, et al. Distinct gene expression profiles in norepinephrine- and epinephrine-producing hereditary and sporadic pheochromocytomas: activation of hypoxia-driven angiogenic pathways in von Hippel–Lindau syndrome. *Endocr Relat Cancer* 2004; **11**: 897–911.
- Bechmann N, Eisenhofer G. Hypoxia-inducible factor 2 α : a key player in tumorigenesis and metastasis of Pheochromocytoma and Paraganglioma? *Exp Clin Endocrinol Diabetes* 2022; **130**: 282–289.
- Jimenez C, Xu G, Varghese J, et al. New directions in treatment of metastatic or advanced Pheochromocytomas and sympathetic Paragangliomas: an American, contemporary, pragmatic approach. *Curr Oncol Rep* 2022; **24**: 89–98.
- Adachi K, Tamada K. Immune checkpoint blockade opens an avenue of cancer immunotherapy with a potent clinical efficacy. *Cancer Sci* 2015; **106**: 945–950.
- Jimenez C, Armaiz-Pena G, Dahia PLM, et al. Endocrine and neuroendocrine tumors special issue-checkpoint inhibitors for adrenocortical carcinoma and metastatic Pheochromocytoma and Paraganglioma: do they work? *Cancers* 2022; **14**: 467.
- Jimenez C, Subbiah V, Stephen B, et al. Phase II clinical trial of Pembrolizumab in patients with progressive metastatic Pheochromocytomas and Paragangliomas. *Cancers* 2020; **12**: 2307.
- Zhang H, Dai Z, Wu W, et al. Regulatory mechanisms of immune checkpoints PD-L1 and CTLA-4 in cancer. *J Exp Clin Cancer Res* 2021; **40**: 184.
- Reck M, Rodríguez-Abreu D, Robinson AG, et al. Pembrolizumab versus chemotherapy for PD-L1-positive non-small-cell lung cancer. *N Engl J Med* 2016; **375**: 1823–1833.
- Tumeh PC, Harview CL, Yearley JH, et al. PD-1 blockade induces responses by inhibiting adaptive immune resistance. *Nature* 2014; **515**: 568–571.
- Galon J, Costes A, Sanchez-Cabo F, et al. Type, density, and location of immune cells within human colorectal tumors predict clinical outcome. *Science* 2006; **313**: 1960–1964.
- Hu H, Chen Y, Tan S, et al. The research Progress of antiangiogenic therapy, Immune Therapy and Tumor Microenvironment. *Front Immunol* 2022; **13**: 802846.
- Jayaprakash P, Vignali PDA, Delgoffe GM, et al. Hypoxia reduction sensitizes refractory cancers to immunotherapy. *Annu Rev Med* 2022; **73**: 251–265.
- Wei J, Hu M, Du H. Improving cancer immunotherapy: exploring and targeting metabolism in hypoxia microenvironment. *Front Immunol* 2022; **13**: 845923.
- Murdoch C, Giannoudis A, Lewis CE. Mechanisms regulating the recruitment of macrophages into hypoxic areas of tumors and other ischemic tissues. *Blood* 2004; **104**: 2224–2234.
- Facciabene A, Peng X, Hagemann IS, et al. Tumour hypoxia promotes tolerance and angiogenesis via CCL28 and T(reg) cells. *Nature* 2011; **475**: 226–230.
- Quinn WJ, Jiao J, TeSlaa T, et al. Lactate limits T cell proliferation via the NAD(H) redox state. *Cell Rep* 2020; **33**: 108500.
- Watson MLJ, Vignali PDA, Mullett SJ, et al. Metabolic support of tumour-infiltrating regulatory T cells by lactic acid. *Nature* 2021; **591**: 645–651.
- Wang ZH, Peng WB, Zhang P, et al. Lactate in the tumour microenvironment: from immune modulation to therapy. *EBioMedicine* 2021; **73**: 103627.
- Guo D, Zhao X, Wang A, et al. PD-L1 expression and association with malignant behavior in pheochromocytomas/paragangliomas. *Hum Pathol* 2019; **86**: 155–162.
- Pinato DJ, Black JR, Trousil S, et al. Programmed cell death ligands expression in phaeochromocytomas and paragangliomas: relationship with the hypoxic response, immune evasion and malignant behavior. *Oncoimmunology* 2017; **6**: e1358332.
- Lam AK y. Update on adrenal Tumours in 2017 World Health Organization (WHO) of endocrine Tumours. *Endocr Pathol* 2017; **28**: 213–227.
- Bernardo-Castiñeira C, Sáenz-de-Santa-María I, Valdés N, et al. Clinical significance and peculiarities of succinate dehydrogenase B and hypoxia inducible factor 1 α expression in parasympathetic versus sympathetic paragangliomas. *Head Neck* 2019; **41**: 79–91.
- Bernardo-Castiñeira C, Valdés N, Celada L, et al. Epigenetic deregulation of Protocadherin PCDHGC3 in Pheochromocytomas/Paragangliomas associated with SDHB mutations. *J Clin Endocrinol Metab* 2019; **104**: 5673–5692.
- Bernardo-Castiñeira C, Valdés N, Sierra MI, et al. SDHC promoter methylation, a novel pathogenic mechanism in parasympathetic paragangliomas. *J Clin Endocrinol Metab* 2018; **103**: 295–305.
- Galon J, Bruni D. Approaches to treat immune hot, altered and cold tumours with combination immunotherapies. *Nat Rev Drug Discov* 2019; **18**: 197–218.
- Gill AJ, Benn DE, Chou A, et al. Immunohistochemistry for SDHB triages genetic testing of SDHB, SDHC, and SDHD in paraganglioma-pheochromocytoma syndromes. *Hum Pathol* 2010; **41**: 805–814.
- Economides MP, Shah AY, Jimenez C, et al. A durable response with the combination of Nivolumab and Cabozantinib in a patient with metastatic Paraganglioma: a case report and review of the current literature. *Front Endocrinol* 2020; **11**: 594264.
- Lim AR, Rathmell WK, Rathmell JC. The tumor microenvironment as a metabolic barrier to effector T cells and immunotherapy. *Elife* 2020; **9**: 1–13.
- Zandberg DP, Menk AV, Velez M, et al. Tumor hypoxia is associated with resistance to PD-1 blockade in squamous cell carcinoma of the head and neck. *J Immunother Cancer* 2021; **9**: e002088.
- Watts D, Bechmann N, Meneses A, et al. HIF2 α regulates the synthesis and release of epinephrine in the adrenal medulla. *J Mol Med* 2021; **99**: 1655–1666.
- Kumagai S, Koyama S, Itahashi K, et al. Lactic acid promotes PD-1 expression in regulatory T cells in highly glycolytic tumor microenvironments. *Cancer Cell* 2022; **40**: 201–218.

42. Wang Y, Johnson KCC, Gatti-Mays ME, et al. Emerging strategies in targeting tumor-resident myeloid cells for cancer immunotherapy. *J Hematol Oncol* 2022; **15**: 118.
43. Talty R, Olinio K. Metabolism of innate immune cells in cancer. *Cancers* 2021; **13**: 904.
44. Lequeux A, Noman MZ, Xiao M, et al. Targeting HIF-1 alpha transcriptional activity drives cytotoxic immune effector cells into melanoma and improves combination immunotherapy. *Oncogene* 2021; **40**: 4725–4735.
45. Cowman SJ, Koh MY. Revisiting the HIF switch in the tumor and its immune microenvironment. *Trends Cancer* 2022; **8**: 28–42.
46. Hsu TS, Lin YL, Wang YA, et al. HIF-2 α is indispensable for regulatory T cell function. *Nat Commun* 2020; **11**: 5055.
47. Kamihara J, Hamilton KV, Pollard JA, et al. Belzutifan, a potent HIF2 α inhibitor, in the Pacak-Zhuang syndrome. *N Engl J Med* 2021; **385**: 2059–2065.
48. Jonasch E, Donskov F, Iliopoulos O, et al. Belzutifan for renal cell carcinoma in von Hippel-Lindau disease. *N Engl J Med* 2021; **385**: 2036–2046.
49. Iacovelli R, Ciccarese C, Procopio G, et al. Current evidence for second-line treatment in metastatic renal cell carcinoma after progression to immune-based combinations. *Cancer Treat Rev* 2022; **105**: 102379.

SUPPLEMENTARY MATERIAL ONLINE

Figure S1. Schematic representation of primary and MPPGL tumor samples analyzed by immunohistochemistry with indicated antibodies